FLOMEKO2019
18th International Flow Measurement Conference
Portugal | Lisbon | LNEC | 26-28 june 2019

The Impact of Geometric Parameters of a S-type Pitot tube on the Flow Velocity Measurement at Smoke-stacks

W. Kang[1], D. T. Nguyen[2], Y-M. Choi[1], S-H. Lee[1]

[1]Korea Research Institute of Standards and Science, Daejeon, Republic of Korea
[2]University of Science and Technology, Daejeon, Republic of Korea
E-mail (corresponding author): woong.kang@kriss.re.kr

Abstract

In the monitoring of greenhouse gas emission from industrial smoke-stacks, the most common device used to measure the stack gas velocity is the S-type Pitot tube in South Korea, which is used to estimate the volumetric flow rate by what is termed the Continuous Emission Monitoring System (CEMS). The S-type Pitot tube installed in the stack is inevitably affected during velocity measurements by velocity changes, yaw and pitch angle misalignments due to the harsh environments. Various geometries of the S-type Pitot tube can affect the characteristics of the S-type Pitot tube coefficients, including the degree of sensitivity to velocity changes and yaw and pitch yaw angle misalignments. Nevertheless, there are no detailed guidelines pertaining to the S-type Pitot tube geometry considering accurate and reliable measurements in the ISO, EPA and ASTM international standards. In the present study, S-type Pitot tubes with various geometric parameters, in this case the distance between the impact and wake orifices and the bending angle of the orifices, were manufactured by a 3D printer. Wind tunnel experiments were conducted in the Korea Research Institute of Standards and Science (KRISS) air speed standard system to determine the optimal geometry of an S-type Pitot tube for the accuracy velocity measurements in actual smokestacks which undergo velocity changes and yaw and pitch angle misalignments. Particle image velocimetry was also used to understand the flow phenomena around an S-type Pitot tube under various geometric and misalignment conditions by means of qualitative visualization.

1. Introduction

GHG emission estimates have been based on an activity-based method (i.e., fuel consumption and emission factors) and on Continuous Emission Monitoring System(CEMS) in the energy sector. The CEMS approach directly measures GHG emissions by monitoring GHG concentrations and volumetric flow rates at the stack. According to the U.S. Environmental Protection Agency (EPA) [1], The CEM method involves estimating the concentrations and flow rates of gas emissions at the stack via following Equation (1).

$$E = \sum_{i=1}^{N} E_{5min,i} = \sum_{i=1}^{N} \left(x_{5min,i} \times Q_{5min,i} \times \frac{M_{gas}}{MV} \right) \quad (1)$$

where $E_{5min,i}$ is the 5-min accumulated emission of the ith measurement (kg), $x_{5min,i}$ is the 5-min averaged concentration of the ith measurement (% or ppm). $Q_{5min,i}$ is the 5-min accumulated volumetric flow of the ith measurement(m^{3}The 5-min accumulated volumetric flow rate can be calculated with following Equation (2).

$$Q_{5min} = V \times \frac{\pi D^2}{4} \times \frac{P_s}{760} \times \frac{273.15}{T} \times (1 - x_w) \times 300 \quad (2)$$

where, Q is the dry gas flow rate (m^3), V is the gas velocity (m/s), D is the stack diameter (m), P_s is the static pressure (mmHg), T is the emission gas temperature (K), and x_w is the water content of the emission gas. The S-type Pitot tube (Stauscheibe or reverse) is most commonly used in the stacks to measure the gas velocity in South Korea.

The S-type Pitot tube was designed to measure the flow velocity for industrial stacks in high-dust environments, as cited in the EPA [2] and ISO standards [3]. This tube design has large pressure orifices and strong tubes, as shown in Figure 1. The flow velocity can be obtained by measuring the differential pressure between the impact orifice and the wake orifice based on the Bernoulli equation. The S-type Pitot tube coefficient (C_p) is used to calculate the flow velocity by measuring the differential pressure with the S-type Pitot tube, as in the following Equation (3).

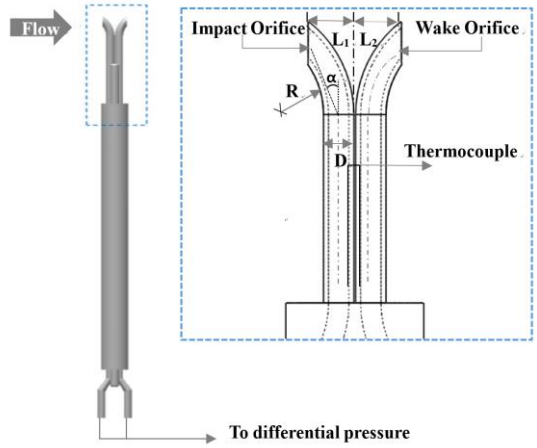

Figure 1: Configuration and definitions of the geometric parameters for the S-type Pitot tube.

$$V = C_P \times \sqrt{\frac{2\Delta P}{\rho}} \qquad (3)$$

where ΔP is the differential pressure (Pa) between the impact and the wake orifices and ρ is the density of the emission gas (kg/m^3).

The S-type Pitot tube is usually installed and inserted in stacks which operate in harsh environments, such as those with tall stack heights and high gas temperatures, as shown in Figure 2. Therefore, it is difficult to observe the inside of the stack and verify the precise installation of an S-type Pitot tube. Accordingly, misalignments, such as yaw angle rotation, can occur during the installation of the S-type Pitot tube from outside of the stack [4]. As the diameter of the stack increases, the sampling point positions for measuring velocity distributions in the stack should increase according to the EPA method [2,3]. Since the inserted length of the S-type Pitot tube also increases, a pitch angle misalignment of the S-type Pitot tube can arise due to the deflection of the tube in stacks with large diameters.

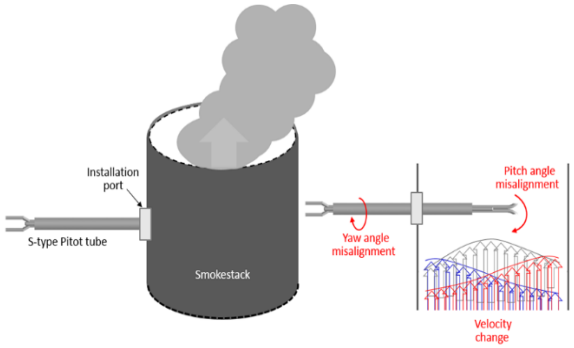

Figure 2: Installation effect of the S-type Pitot tube in the stack.

Table 1: Specifications parameters of an S-type Pitot tube recommended in the international standards

Parameter	ASTM D3796	ISO10780	EPA Method 2
D	-	4 mm to 10 mm	4.8 mm to 9.5 mm
α	45°	-	-
$L=L_1=L_2$	9.52 mm	1.05D to 10D	1.05D to 1.5D

This would affect not only the velocity change but also the yaw and pitch angle flow to the S-type Pitot tube installed in the stack. Hence, an S-type Pitot tube installed in the stack is inevitably affected during velocity measurements by the velocity change, yaw and pitch angle misalignments due to the reasons described above (Figure 2).

If the geometry of the S-type Pitot tube is less sensitive to changes in the flow velocity and to yaw and pitch angle misalignments, flow velocity measurements by S-type Pitot tubes in the stack can be more accurate. From the international documents related to S-type Pitot tubes, specifically ISO, ASTM and EPA [3,5,6], the geometric parameters of S-type Pitot tubes, in this case the external diameter, the half of distance between the impact and wake orifices (L), and the bending angle of the orifices (α), as shown in Figure 1, are defined and described in Table 1. However, the values of geometric parameters are described differently in the documents, specifically the range of the distance between the two orifices(L) and the bending angles(α) of orifices. Various geometries of S-type Pitot tubes can affect the characteristics of the S-type Pitot tube coefficients, including the sensitivity to velocity changes and pitch and yaw angle misalignments. However, there are no detailed guidelines for S-type Pitot tube geometries considering accurate and reliable measurement characteristics in the international standards.

The main objective of the present study is to determine the optimal geometry of an S-type Pitot tube for accurate and reliable velocity measurements in an actual stack considering velocity changes and yaw and pitch angle misalignments. To this end, S-type Pitot tubes with various geometric parameters, in this case the distance (L) and the bending angle (α) of the orifices, were manufactured by a 3D printer. Wind tunnel experiments were conducted in KRISS air speed standard system to determine the effects of the geometric parameters on the S-type Pitot tube coefficients with change in the velocity and yaw and pitch angles. Particle image velocimetry was also utilized to understand the flow phenomena around an S-type Pitot tube under various geometric and misalignment conditions by means of qualitative visualizations.

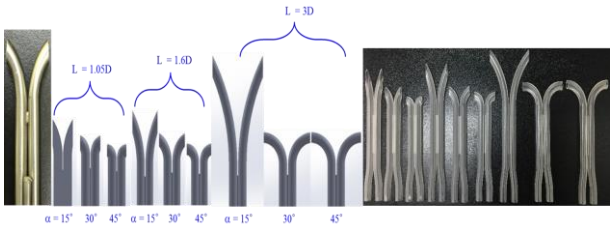

Figure 3: 3D printed S-type Pitot tube models with various geometric parameters.

2. Experimental method and apparatus

2.1 Geometric Parameters of the S-type Pitot tubes

In order to investigate the effects of the geometry of an S-type Pitot tube on the accuracy of flow velocity measurements in the stack, the various geometric parameters of the S-type Pitot tube were designed. In the present study, the values of the half of distance between the impact and wake orifices, *L*, were set to 1.05*D*, 1.6*D* and 3*D*. The used S-type Pitot tube in KRISS has 30° as the bending angle(α), which differs from the bending angle of 45° described in ASTM. The three different bending angle, 15°, 30° and 45° were selected for S-type Pitot tube models. Each combination consisted of S-type Pitot tube models with these three distances (*L*=1.05*D*, 1.6*D* and 3*D*) and with bending angles α of 15°, 30° and 45°, as shown in Figure 3. To manufacture the designed S-type Pitot tube models with various geometric parameters, a 3D printer, which relies on a stereo lithography method, was used in the Daejeon Techno-Park with an ATOMm-4000 3D Printer.

2.2 Experimental in a wind tunnel system

To evaluate the effect of a change in the velocity and the yaw and pitch angle misalignments on the manufactured S-type Pitot tube models, wind tunnel tests were conducted in the subsonic open-circuit wind tunnel of KRISS, which was used as national air speed standards, as shown in Figure 4. The dimensions of the test section were 900 mm (width) × 900 mm (height) × 6000 mm (length). The inlet velocities were varied from 2 m/s to 16 m/s. The turbulent intensity in the test section is less than 0.5 %. The expanded uncertainty levels (*U*) of the flow velocity measurements in the KRISS wind tunnel standards system is less than 1.1 % from 2 – 5 m/s and 0.6 % from 5 – 15 m/s at the 95 % confidence level.

The experimental setup was arranged as shown in Figure 4, and all of the data were acquired automatically by the LabVIEW program. Additionally, to alter the yaw and pitch angle of the S-type Pitot tube, a rotating device was installed at the top of the test section.

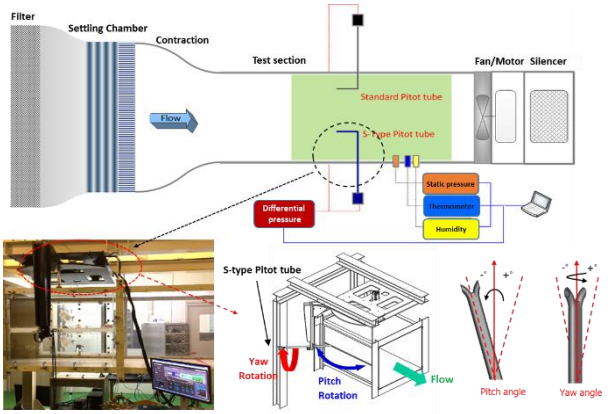

Figure 4: Experimental set-up of the S-type Pitot tube models in the KRISS wind tunnel.

With this rotating device, the yaw angles could change from -180° to +180° at an interval of 1°, while the pitch angles could change from -45° to +45° at 5° intervals. In addition to experiments in the wind tunnel system, to understand the flow phenomena around the S-type Pitot tube models when the velocity, yaw and pitch angle change, qualitative visualization experiments were also conducted using a particle image velocimetry (PIV) system. A laser light sheet was produced by a time-resolved laser that delivered 20mJ of energy per pulse at 1kHz. Tracer particles in the flow fields were seeded by a seeding generator. Particle images were captured by a 50mm lens (Zeiss) and a 12-bit high-speed camera (SpeedSense M310) at 1280 x 800 pixels. The field of view was 150 mm x 100 mm. For each geometry of the S-type Pitot tube models, 5000 instantaneous PIV images were acquired using Dynamic Studio (Dantec Dynamics).

3. Results and discussions

3.1 The effect of the velocity changes on the S-type Pitot tube coefficients

To investigate the effects of the geometries of the S-type Pitot tube models on the S-type Pitot tube coefficients when the incoming velocity at the orifice of the S-type Pitot tube changes, wind tunnel experiments with S-type Pitot tubes were conducted at a velocity range of 2 to 15 m/s. The upper part of Figure 5 shows the distribution of the S-type Pitot tube coefficients with respect to velocity changes for *L*=1.6*D* and α=15˚, 30˚ and 45˚. In particular, the distribution of the S-type Pitot tube coefficients with *L*=1.6*D* and α=45˚ has large coefficients when the incoming velocity increases as compared to when α=15˚ and 30˚ despite the identical distance (*L*) between the two orifices. To understand this result, the flow phenomena around the S-type Pitot tube

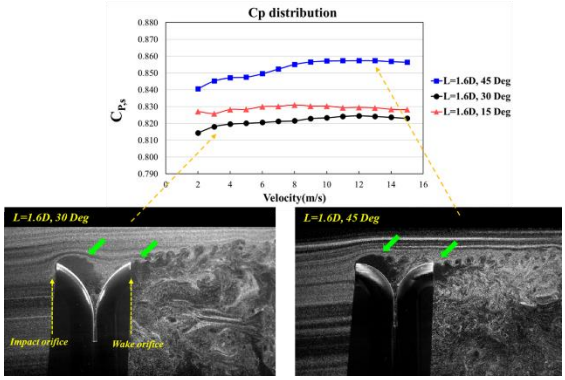

Figure 5: Distribution of S-type Pitot tube coefficients and flow visualization by PIV when L=1.6D and α=15˚, 30˚ and 45˚.

models with L=1.6D, α=30˚ and 45˚ were investigated by PIV measurements, as shown in the bottom of Figure 5. Due to complicated geometry between the impact and wake orifices, the separated flows were developed to a vortical structure behind the impact orifices. For the case of L=1.6D and α=30°, the separated flow develops to the vortical structures behind the impact and the wake orifices of the model. In contrast, in the case of L=1.6D and α=45°, downstream separated flows from wake orifice were less developed than when α=30° due to short distance between two orifices and a gradual change of curved shape. Accordingly, the lower pressure distribution was presented around the wake orifice. It causes the S-type Pitot tube coefficients for the case of L=1.6D and α =45° decreased as shown in the upper part of Figure 5.

In the flow phenomena between the two orifices of the S-type Pitot tube models in Figure 5, it can be seen that the actual contact distance of the flow between the two orifices is more important than the distance L as defined above when determining the S-type Pitot tube coefficients with respect to velocity changes. Therefore, the actual contact distance of the flow between the impact and wake orifice was introduced to examine the effects of the geometries of the S-type Pitot tube models on the S-type Pitot tube coefficients. In the present study, it was termed an effective length, eL, as shown in Figure 6.

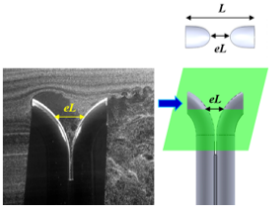

L (mm)	α (°)	eL (mm)	eL/D
1.05D	15	10.16	1.06
	30	6.54	0.68
	45	3.16	0.32
1.6D	15	20.68	2.16
	30	15.90	1.66
	45	8.76	0.92
3D	15	47.64	4.98
	30	41.82	4.38
	45	26.64	2.78

Figure 6: Definition of the effective length (eL) of the S-type Pitot tube.

As shown in Figure 6, the normalized effective length (eL/D) when L=1.6D and α= 45° is shortest among all model with the same distance of L=1.6D. This indicates that the interference between the impact and wake orifice in the separated flow were stronger than in the other models with longer effective lengths.

Since the S-type Pitot tube as utilized in the stack uses the average value of the S-type Pitot tube coefficients within the velocity ranges, the more constant the coefficient within the entire range of velocity changes is, the more accurate the velocity measurements can be achieved. This can be determined by the standard deviation of the coefficients with respect to the change in the velocity. In addition, the recommended value of S-type Pitot tube coefficient, 0.84 was described in ISO 10780 [3]. Accordingly, the uncertainty due to S-type Pitot tube coefficients with respect of incoming velocity change can be assessed by Equation (4).

$$u_{C_p} = \sqrt{\sigma_{C_p}^2 + \frac{(C_p - 0.84)^2}{2\sqrt{3}}} \qquad (4)$$

Figure 7 shows the uncertainty of S-type Pitot tube coefficients with respect to the normalized effective length (eL/D) for all nine S-type Pitot tube models, which calculated by Equation (4). It is interesting to note that uncertainty of the S-type Pitot tube coefficients decreases as the effective length increases. This implies that S-type Pitot tube models with long effective lengths have more constant distributions of the S-type Pitot tube coefficients with respect to velocity changes. When the effective length(eL/D) is larger than 0.8 in the Figure 7, the S-type Pitot tube models have lower uncertainty level that ISO's recommended value. It means that we can suggest geometric parameter of S-type Pitot tube, in this case, the effective length range for the constant distribution of S-type Pitot tube coefficients with respect to incoming velocity.

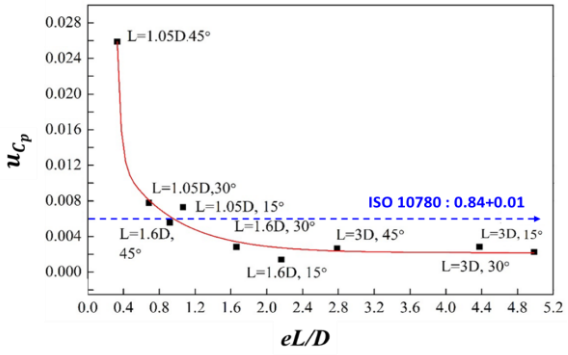

Figure 7: Uncertainty of S-type Pitot tube coefficients with respect to normalized effective length.

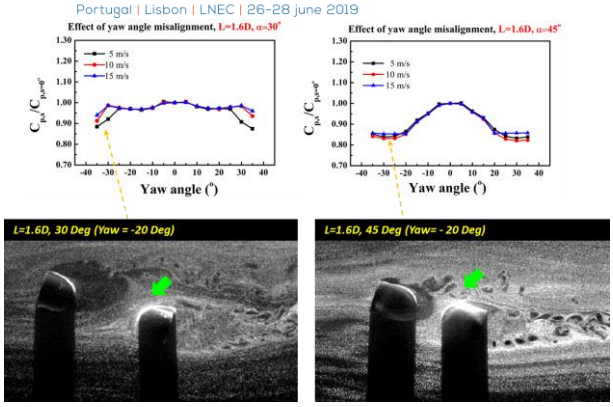

Figure 8: Distribution of S-type Pitot tube coefficients and flow visualization by PIV when L=1.6D with yaw angle change.

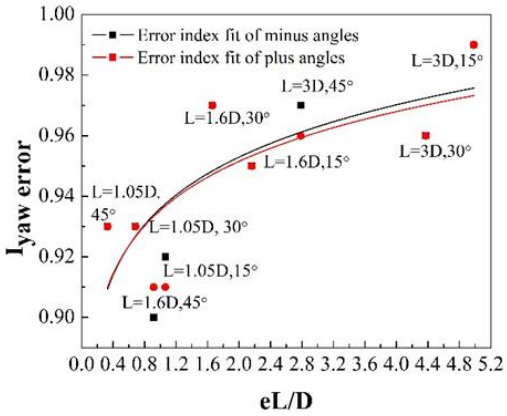

Figure 9: Yaw angle misalignment error indexes of S-type Pitot tube models with various geometries.

3.2 The effect of yaw and pitch angle misalignments on the S-type Pitot tube coefficients

To elucidate the effect of the geometries of the S-type Pitot tube models on the S-type Pitot tube coefficients under the yaw and pitch angle misalignments, wind tunnel experiments were conducted with various geometries of the S-type Pitot tube models. The yaw and pitch angle ranges varied from -35° to +35° within a velocity range of 2 to 15 m/s.

When L=1.6D, α=30° and 45°, the distributions of the S-type Pitot tube coefficients were considerably different, as shown in the upper part of Figure 8. PIV measurements were conducted for the flow phenomena around the S-type Pitot tube models with L=1.6D, α=30˚ and 45˚ with yaw angle misalignment of -20 ˚. The lower and right part of Figure 8 shows that the separated flows from the surface of the impact orifices interfere with vortical structures separated from the wake orifice when L=1.6D and α=45˚. This causes the pressure distributions near the wake orifice to drop sharply. Thus, the normalized coefficient values of the model with L=1.6D and α=45˚ tended to decline dramatically upon yaw angle misalignments. On the other hand, in the case of L=1.6D and α=30˚, there is no interference between the separated flows from the impact orifice and the flows near the wake orifice due to the long distance between the two orifices. It is interesting to note that the actual contact distance of the flow between the two orifices is also an important parameter when determining the effect of yaw angle misalignments.

To quantify the effects of the geometry of the S-type Pitot tube models on the S-type Pitot tube coefficients during yaw angle misalignments, an error index, $I_{yaw\ error}$, was defined by using the ratio of area between yaw normalized curve and curve at yaw=0˚. It is determined by the Equation (5).

$$I_{yaw\ error} = \frac{Area\ of\ yaw\ normalized\ curve}{Area\ of\ curve\ at\ yaw=0^{\circ}} \quad (5)$$

Area of yaw normalized curve is the area under the curve for the normalized S-type Pitot tube coefficients with respect to the yaw angle misalignment. Area of curve at yaw=0 ° is the area under the curve for the normalized S-type Pitot tube coefficients with no yaw angle misalignment, which is $C_{p,s}/C_{p,s}$=0˚. When error index, $I_{yaw\ error}$, closed to the 1, it indicates that the S-type Pitot tube models were less affected by the yaw angle misalignments.

Figure 9 shows the error index of yaw angle misalignments, $I_{yaw\ error}$, for S-type Pitot tube models with various geometric parameters. The positive and negative yaw angles show almost similar tendency as shown in the error index fit of all S-type Pitot tube models. It is interesting to note that the error index of the S-type Pitot tube models becomes close to 1 as the normalized effective length, eL/D, increases. This means that S-type Pitot tube models with long effective lengths are less affected by the yaw angle misalignments.

Unlike yaw angle misalignment, the S-type Pitot tube coefficients when negative and positive pitch angle misalignments are not symmetric. Therefore, in the case of negative pitch angle misalignments, the error index, $I_{pitch\ error}$ is smaller than 1. On the other hand, in the case of positive pitch angle misalignments, the error index is larger than 1. When error index, $I_{pitch\ error}$, closed to the 1, it means that the S-type Pitot tube models were less affected by the pitch angle misalignments. Figure 10 shows the error indexes of pitch angle misalignments for S-type Pitot tube models with various geometric parameters. It is interesting to note that the effective length of S-type Pitot tube coefficients were not correlated with the error index, which shows similar values of error indexes except for small effective length, eL/D<0.1 in the negative pitch angle.

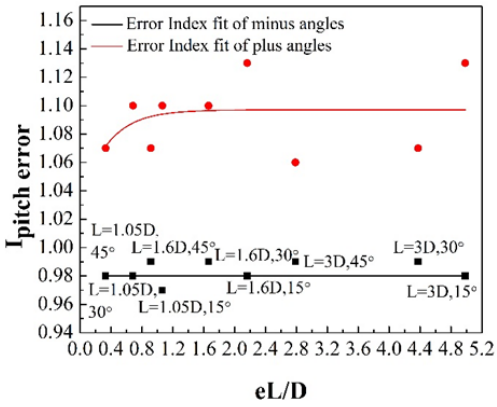

Figure 10: Pitch angle misalignment error index of S-type Pitot tube models with various geometries.

4. Conclusion

The main objective of the present study is to determine the optimal geometry of an S-type Pitot tube so as to improve the accuracy of velocity measurements in actual smokestacks which undergo velocity changes and yaw and pitch angle misalignments. The wind tunnel experiments and PIV measurements for the S-type Pitot tube coefficients of models with various geometries show that the distributions of the coefficients with respect to incoming velocity are related to certain flow phenomena, in this case separated flows and voritical structures around the impact and wake orifices. An S-type Pitot tube coefficient with a long effective length, *eL/D* has more constant distributions of the S-type Pitot tube coefficients and lower uncertainty when the velocity changes from 2 m/s to 15 m/s. Therefore, we can suggest geometric parameter, in this case, the effective length range for the constant distribution of S-type Pitot tube coefficients with respect to incoming velocity.

The distributions of S-type Pitot tube coefficients upon yaw and pitch angle misalignments differed depending on the combination of geometric parameters for the distance (L) and the bending angle (α). The actual contact distance of the flow between the two orifices, effective length is also an important parameter when determining the effects of yaw angle misalignments, similar to the effects of velocity changes. The error index, $I_{yaw\ error}$ for yaw angle misalignments shows that S-type Pitot tube models with long effective lengths are less affected by yaw angle misalignments. However, the use of S-type Pitot tube with long distance length is impractical due to the hole size in the smoke-stack for installing S-type Pitot tube. Therefore, we can suggest the certain effective length of S-type Pitot tube considering both the sensitivity to yaw angle misalignment and the practical use in the smoke-stack. On the other hand, the S-type Pitot tube coefficients were mostly insensitive to the both of positive and negative pitch angle misalignments regardless of the velocity and geometry of the various models. The error index for pitch angle misalignment shows that the S-type Pitot tube coefficients were not correlated with the effective length given the similar value of error indexes except for small effective length, $eL/D<0.1$ in the negative pitch angle.

References

[1] U.S. Environmental Protection Agency, *Greenhouse Gas Reporting Program 40 CFR 98.30 Subpart C*, 2013

[2] U.S. Environmental Protection Agency. *Determination of stack gas velocity and volumetric flow rate (type S Pitot tube), EPA method 2*, 2000

[3] ISO 10780: *Stationary source emissions – Measurement of velocity and volume flowrate of gas streams in ducts*, 1994

[4] Kang W, Trang N D, Lee S H, Choi H M, Shim J S, Jang H S, Choi Y M, "Experimental and numerical investigations of the factors affecting the S-type Pitot tube coefficients" *Flow Meas. Instrum.*, 44, 11-18, 2015.

[5] U.S. Environmental Protection Agency, *Determination of stack gas velocity and volumetric flow rate (type S Pitot tube). US Environmental Protection Agency, Part 60 Appendix A, Method 2*, 1971.

[6] ASTM D3796-90: *Standard practice for calibration of Type S Pitot tube*, 2004.